Fall 2012

Verification of a Monte Carlo model of the Missouri S&T reactor

Brad Paul Richardson

VERIFICATION OF A MONTE CARLO MODEL OF THE MISSOURI S&T REACTOR

by

BRADLEY PAUL RICHARDSON

A THESIS

Presented to the Faculty of the Graduate School of the

MISSOURI UNIVERSITY OF SCIENCE AND TECHNOLOGY

In Partial Fulfillment of the Requirements for the Degree

MASTER OF SCIENCE IN NUCLEAR ENGINEERING

2012

Approved by

Carlos H. Castano, Advisor
Shoaib Usman
Hyoung K. Lee

ABSTRACT

The purpose of this research is to ensure that an MCNP model of the Missouri S&T reactor produces accurate results so that it may be used to predict the effects of some desired upgrades to the reactor. The desired upgrades are an increase in licensed power from 200 kW to 400kW, and the installation of a secondary cooling system to prevent heating of the pool. This was performed by comparing simulations performed using the model with experiments performed using the reactor. The experiments performed were, the approach to criticality method of predicting the critical control rod height, measurement of the axial flux profile, moderator temperature coefficient of reactivity, and void coefficient of reactivity. The results of these experiments and results from the simulation show that the model produces a similar axial flux profile, and that it models the void and temperature coefficients of reactivity well. The model does however over-predict the criticality of the core, such that it predicts a lower critical rod height and a k_{eff} greater than one when simulating conditions in which the reactor was at a stable power. It is assumed that this is due to the model using fuel compositions from when the fuel was new, while in reality the reactor has been operating with this fuel for nearly 20 years. It has therefore been concluded that the fuel composition should be updated by performing a burnup analysis, and an accurate heat transfer and fluid flow analysis be performed to better represent the temperature profile before the model is used to simulate the effects of the desired upgrades.

ACKNOWLEDGMENTS

I would like to thank my Advisor, Dr. Carlos Castaño for his patience and guidance in helping me to earn my degree. I would also like to thank Dr. Jeffrey King, without whom's previous work, this research would not have been possible. I would like to thank Dr. Shoaib Usman and Dr. Ayodeji Alajo for their help with this project as well.

I would like to acknowledge my sources of funding, which included the Chancellor's Fellowship, funding from the Nuclear Engineering Department, and the NANT Fellowship. I would like to thank Dr. Arvind Kumar for his assistance in procuring this funding.

I would like to thank the members of my committee, Dr. Carlos Castaño, Dr. Shoaib Usman, and Dr. Hyoung-Koo Lee, for their time and energy.

Finally, I would like to thank my Parents and Grandparents for all their support and funding in the course of my education.

TABLE OF CONTENTS

LIST OF ILLUSTRATIONS

Page

LIST OF TABLES

Page

1. INTRODUCTION

1.1. BRIEF HISTORY OF MSTR

The Missouri S&T Reactor has been in operation since 1961 and was the first reactor built in Missouri (Missouri S&T Nuclear Reactor, 2008). The MSTR began its operation with highly enriched uranium (HEU) fuel. The fuel was exchanged for low enriched (LEU) fuel, at approximately 19.9% U-235, in 1992 (Bonzer, 2011).

1.1.1. Facilities. The reactor core is positioned near the bottom of a 32,000 gallon pool with dimensions 9 ft. wide, 19 ft. long and 27 ft. deep (Missouri S&T Nuclear Reactor, 2008). It includes a 30 ft. deep spent fuel storage area with a large concrete bulk head separating it from the rest of the pool. The core hangs from a bridge above the pool which rests on wheels, allowing the reactor to be moved along the length of the pool. The water is processed using a filter and demineralizer to keep it clean and reduce corrosion on the components in the pool. There is also a skimming device at the top of the pool to remove detritus from the water in the pool.

The current core configuration, referred to as "120W", consists of 15 fuel elements containing 18 fuel plates, and 4 control rod elements with the 8 middle plates excluded to accommodate the control rods. Diagrams of the fuel elements are shown in Figures 1.1 and 1.2. The elements are 3 in. by 3 in. by 3 ft. long, with a cylinder at the bottom which fits into the grid plate on which the core rests (Safety Analysis Report For The University of Missouri-Rolla Reactor, 1988). Three of the control rods are stainless steel 304 (SS304) alloyed with natural boron (shim rods) and are used for coarse control, shutdown, and SCRAM. The fourth control rod, called the regulating rod, consists of standard SS304 and is used for fine control. A picture of the reactor is shown in Figure 1.3.

The fuel in the MSTR is low-enriched Uranium Silicide clad in Aluminum. The fuel plates are 0.06 in. thick and curved to allow for thermal expansion during operation, and extend more than 24 in. within the element to allow for 24 in. of active fuel height (Safety Analysis Report For The University of Missouri-Rolla Reactor, 1988).

There is a Plutonium-Beryllium neutron source which can be placed near the core in an aluminum cylinder and is used for startup and low power operations.

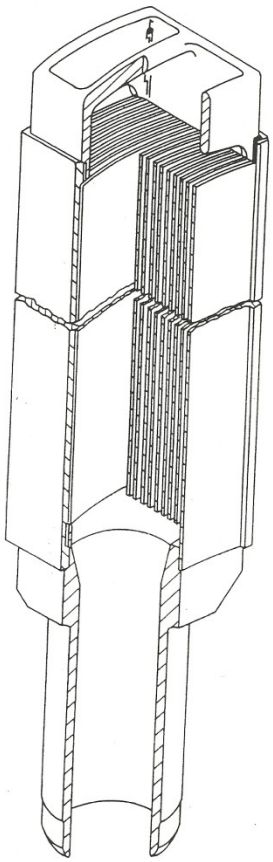

Figure 1.1. Diagram of a Fuel Element.

There are several irradiation facilities available. The thermal column is a large, 3.5 ft. by 3.5 ft. by 5 ft. graphite block at the rear of the pool with holes in the back of it, which is a good source for thermal neutrons (Missouri S&T Nuclear Reactor, 2008). The core can be positioned closer or further from the thermal column and is denoted in the core configuration by either a T for thermal or W for water mode.

The beam port is a 6 in. diameter aluminum tube which extends from near the core to a room in the reactor building basement (Missouri S&T Nuclear Reactor, 2008). It has a lead shield which can be opened to provide a beam of neutrons into the basement.

There are two "rabbit tubes" which can be used to quickly insert and remove samples from the core (Missouri S&T Nuclear Reactor, 2008). There is a small box in the reactor bay into which the samples are loaded and compressed nitrogen is used to force the sample to and from the core. One rabbit tube is lined with cadmium to prevent

thermal neutrons from reaching the sample, hence providing irradiation of epithermal and fast neutrons only.

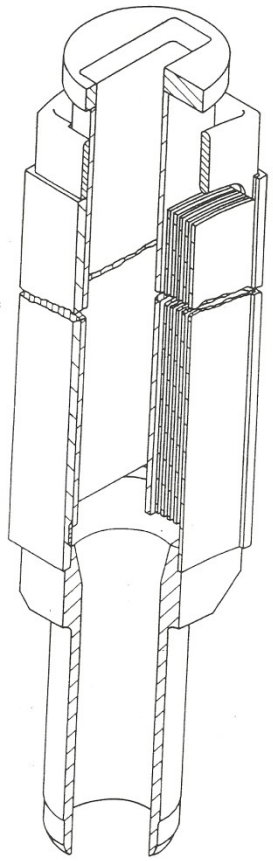

Figure 1.2. Diagram of a Control Element.

There are also several void tubes into which samples can be loaded. The void tubes are large aluminum tubes which fit into a grid spacing, usually used for long term exposures or large samples which do not fit into the rabbit tubes. A diagram of a void tube is shown in Figure 1.4.

1.1.2. Instrumentation. There are several different detectors and monitors used to keep track of the power of the reactor. When the reactor is at low power it is monitored using a fission chamber (Safety Analysis Report For The University of Missouri-Rolla Reactor, 1988). The fission chamber can be raised away from the core

into a shielded container to protect it and extend its life during higher power operations. It is calibrated to accurately measure the power level of the reactor when it is fully lowered near the core.

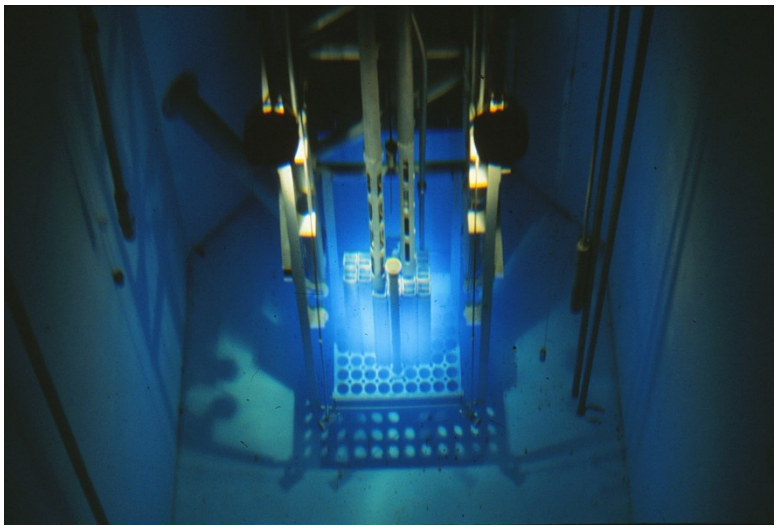

Figure 1.3. Picture of the Reactor From the Top of the Pool (Missouri S&T Nuclear Reactor, 2008).

There are two compensated ion chambers used to monitor the power level of the reactor during mid-range power level operations (Safety Analysis Report For The University of Missouri-Rolla Reactor, 1988). The voltage applied to the detectors can be changed in discrete steps to display the power level of the reactor as a percentage of a certain power level. The steps are 20 W, 200 W, 2 kW, 20 kW, and 200 kW. The measurements of these detectors and the fission chamber are recorded on rolls of paper by a moving pen.

There are also two uncompensated ion chambers used to monitor the power level of the reactor. These detectors are used only for high power operations and are calibrated to display the power level as a percentage of full power (200 kW) (Safety Analysis Report For The University of Missouri-Rolla Reactor, 1988).

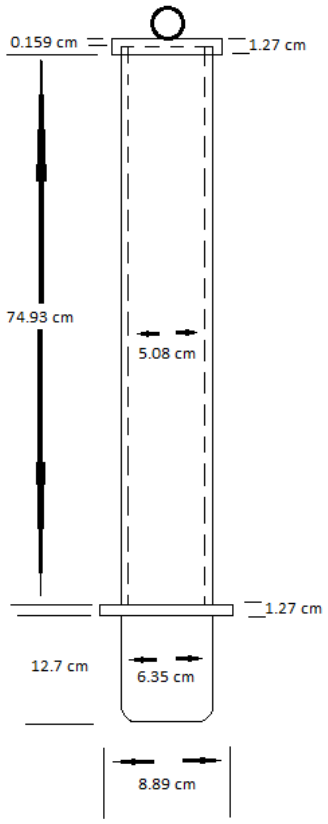

Figure 1.4. Diagram of a Void Tube.

There is also a device which displays the period of the reactor, or the time in which it would take the reactor to double in power if left in its current state. The period is recorded on the same roll as the compensated ion chamber. All of these instruments are connected to a number of indicator lights which will illuminate and sound an alarm in the presence of certain situations. Many of these situations will cause an automatic response from the reactor controls. These can be either a loss of ability to remove control rods any further, an automatic gradual reinsertion of the control rods, or a SCRAM (immediate drop of the control rods from their mechanism back into the core) (Safety Analysis Report For The University of Missouri-Rolla Reactor, 1988).

There are four thermocouples which give readings in the control room. Two of these are positioned just below the core, one is positioned 5 ft. above the core, and one measures the temperature in the reactor bay (Safety Analysis Report For The University

of Missouri-Rolla Reactor, 1988). There are also 4 radiation area monitors throughout the building. One is on the bridge (support above the pool from which the core hangs) one is near the demineralizer, one is in the room near the beam port, and one is near the large exhaust fan in the bay.

1.1.3. New Upgrades. There have been a few recent upgrades made to the reactor. One upgrade involved rearranging the fuel elements in the core and repositioning it in order to increase the neutron flux in the beam port. Another is the addition of a new irradiation facility. This facility includes a core delivery system similar to the rabbit tubes. Also there are two shielded hot cells into which this system can deliver samples. One is a storage area which can hold and automatically retrieve up to 16 samples. The other includes a number of detectors which can be used to measure the activity of the sample. The entire system is controlled remotely via a computer system (Grant, Mueller, Castano, Kumar, & Usman, 2010).

1.2. PRESENT FUEL AND CORE CONFIGURATION

The current fuel was installed in 1992 and has been used for operations since that time. At the time it was installed the enrichment of the fuel was approximately 19.9% U-235. The reactor was relicensed by the NRC in 2008. The configuration of the core was changed recently to 120W and its position was moved to line it up with the beam port. This means the grid plate is positioned approximately 6 in. from the thermal column. A map of the core is shown in Figure 1.5.

1.3. MSTR CAPABILITIES

The Missouri S&T Reactor (MSTR) is primarily a teaching reactor. Nuclear Engineering students at Missouri S&T learn how to operate the MSTR and many obtain an NRC Reactor Operator license for the MSTR. Additionally, students perform experiments using the reactor to learn various physical principles pertaining to reactor physics, as well as some fundamental nuclear engineering principles. Many of the concepts learned can be extended to commercial and/or other experimental reactors. The

MSTR is also equipped with several irradiation facilities for various irradiation experiments. The most recent addition is the internet accessible hot-cell facility (Grant, Mueller, Castano, Kumar, & Usman, 2010), which makes the reactor available to distance users. Other irradiation facilities include the rabbit tubes, neutron beam port, and void tubes (Missouri S&T Nuclear Reactor, 2008). These irradiation facilities are currently available to both campus and distance users.

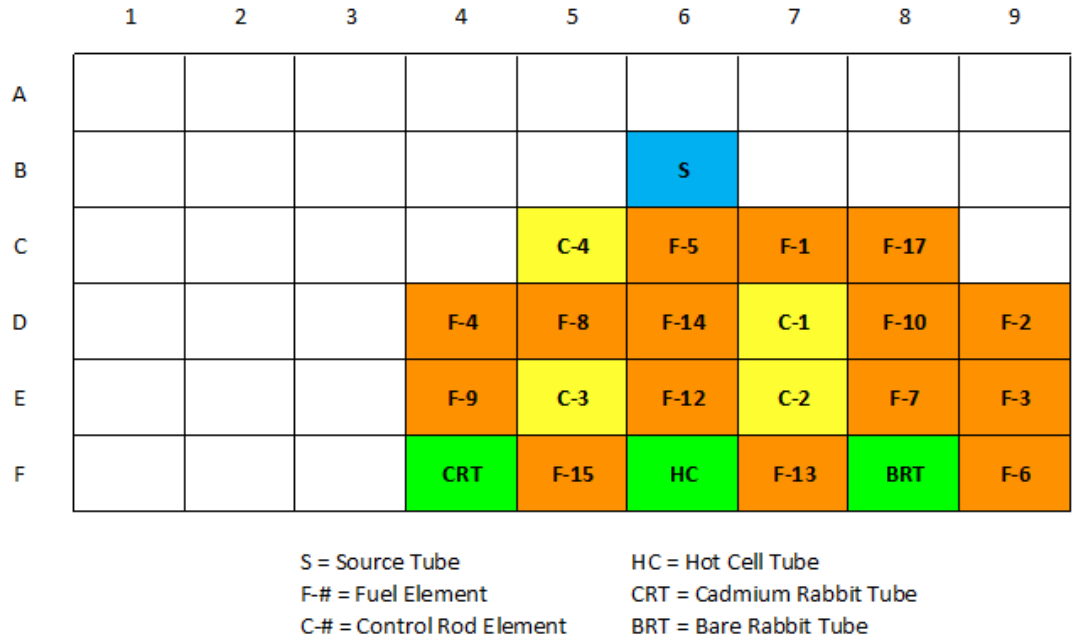

Figure 1.5. Map of 120W Core Configuration.

The reactor has a maximum licensed power of 200 kW, providing a maximum flux of nearly 10^{12} neutrons/cm^2/sec (Safety Analysis Report For The University of Missouri-Rolla Reactor, 1988). If the reactor has been run at high power it can be shutdown to provide a source of only gamma radiation as well.

1.4. LIMITATIONS AND DESIRED UPGRADES

The MSTR has a maximum licensed power of 200 kW, providing a maximum total flux of $4.36 \times 10^{12} \pm 2.84 \times 10^{11}$ neutrons/cm^2/s at the bare RABBIT tube (Bonzer, 2011). The reactor is currently staffed during weekdays from 8 am to 5 pm. The MSTR is operated intermittently during those hours as needed and is shutdown every afternoon and restarted the following morning. This means that it is not possible to irradiate a sample for longer than 9 hours, resulting in a maximum single irradiation neutron fluence of about 1.41×10^{17} neutrons/cm^2.

If the reactor is operated at full power for an extended period of time, the water in the pool begins to heat up. The increase in temperature necessitates the removal of control rods to keep the reactor critical and eventually the reactor will not be able to continue to operate.

In order to address these limitations, Missouri S&T is pursuing an increase in licensed power and the installation of a secondary cooling system using support from a Nuclear Energy University Partnership (NEUP) Reactor Upgrade Grant. The goal of the present study is to develop and validate a high quality computer model of the MSTR which will enable neutron flux predictions at various irradiation facilities, as well as support the licensing of a future reactor power upgrade. A schematic of the intended secondary cooling system is shown in Figure 1.6.

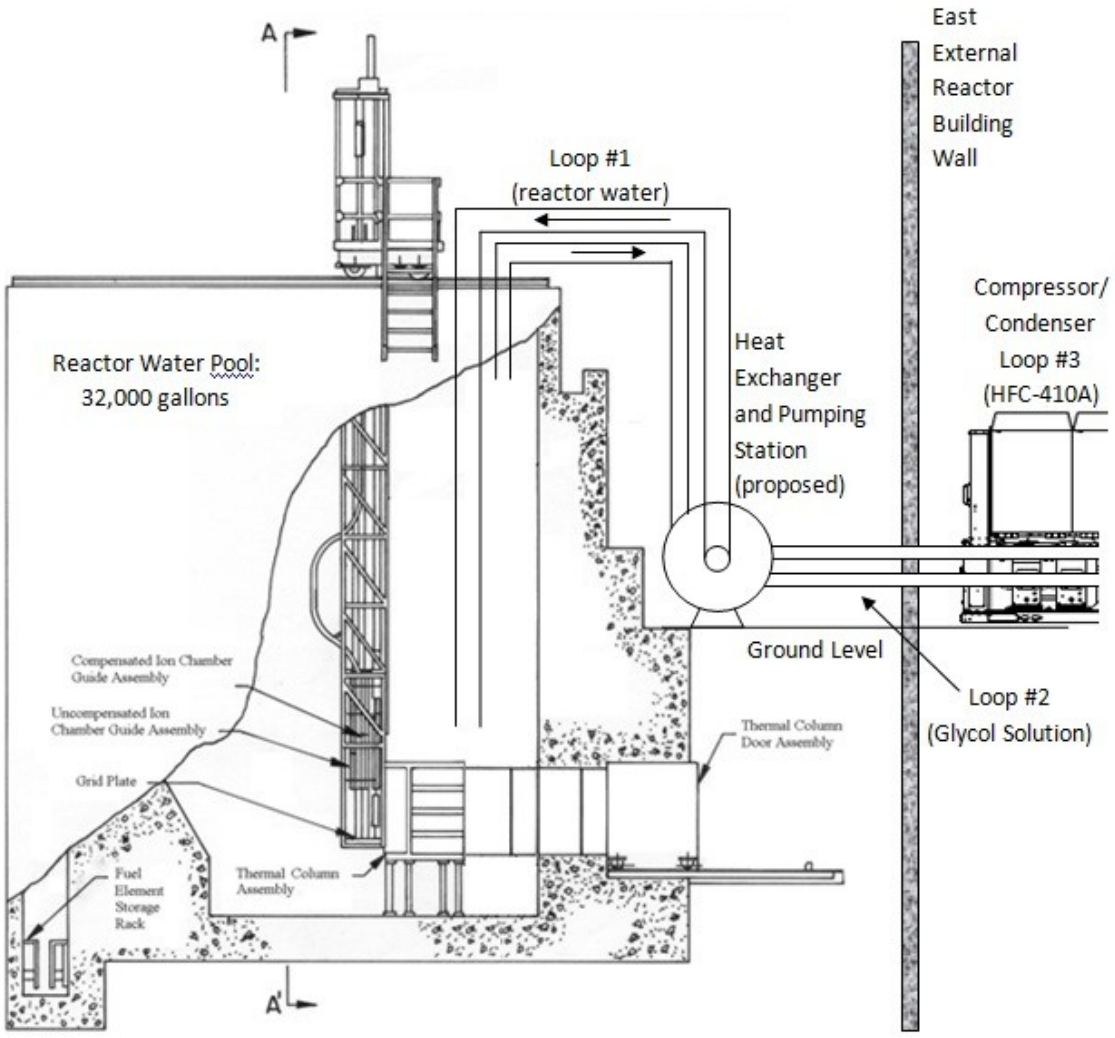

Figure 1.6. Schematics for Desired Secondary Cooling System.

2. MODELING

2.1. MCNP

MCNP is a computer program developed by Los Alamos National Lab for simulating neutron environments (Los Alamos National Laboratory, 2008). The program uses a Monte Carlo method for modeling systems. The input for the program is a description of the geometry of the environment using surfaces to define cells and material definitions for what those cells consist of. The surfaces are infinite planes or cylinders, spheres, or some macro bodies such as toroids or parallelepipeds. The cells are then defined as some combination of these surfaces with respect to which side of the surface. The cell is then defined as consisting of some material at some density. The material is defined as containing some particular mixture of isotopes.

A definition of the source of particles is also required. This definition includes where, with what energy, and headed in what direction each particle starts and with what frequency the particles are started with those characteristics. Finally a description of desired output from the program is defined. This usually consists of a number of tallies for determining flux values at particular locations. The program then uses a library of energy dependant cross sections and the material definitions to calculate macroscopic cross sections for all possible particle interactions within each cell.

The particles are started according to the source definition and tracked through the system. The particle undergoes interactions according to probabilities determined from the cross sections calculated from the material definitions. The particle is tracked until it has an absorption or fission interaction or leaves the system.

The program may also be run in "kmode," so that the effective multiplication factor (k_{eff}) of the system may be calculated. The program starts the particles in cycles. For the first cycle the particles are started according to the defined source. For each subsequent cycle the particles are started at the sites where fission interactions occurred in the previous cycle. The k_{eff} of the system is then the number of neutrons produced from fission divided by the number of neutrons started in the cycle.

2.2. MODEL DEVELOPMENT

The original model of the Missouri S&T Reactor was developed in 2007-08 by Dr. Jeffrey King. The model represents the actual geometry of the core as near as was possible. The dimensions were taken from a combination of blue prints, shipping papers and some visual inspection. The model includes the whole reactor pool, thermal column, spent fuel storage pit, and the part of the beam port that extends into the pool as well as the core. While the model includes the concrete structures outside of the reactor pool, these regions are assigned an importance of zero, ending neutron tracking at the edge of the reactor pool. The core includes all of the fuel elements, the rabbit tubes, the control rods, and the grid plate on which the core rests. The support structure above the core was not included in the model.

The model was also written in such a way that elements of the core which are moveable are easily changed in the model. Control rod heights may be changed individually using a transform for each. Each fuel element is written as its own universe and placed using one of the transforms written for each grid space within the core. Since the core is on rails and may be moved along the length of the pool, a transform was also written to allow horizontal positioning of the core. This flexibility of horizontal movement allows the model to be easily changed from “T” mode to “W” mode and vice versa.

The material compositions for the reactor components were taken from blueprints and shipping papers. The fuel composition for each fuel element is based on the shipping documents received by the reactor during the conversion from highly-enriched uranium fuel to the current low-enriched uranium fuel. The aluminum cladding and other aluminum pieces use compositions reported in the quality control reports. The concrete, stainless steel, and borated stainless steel compositions are based on examples in the MCNP Primer (Brewer, 2009). The 1100-series aluminum compositions come from MatWeb (MatWeb, 1996-2011). Lead, cadmium, water and graphite were taken to have naturally occurring isotopic compositions as reported in the chart of nuclides (Lockheed Martin, 2002). Table 2.1 shows the resulting isotopic compositions of the materials used in the model.

Table 2.1. Table of Composition of Materials Used in the Model.

Material	Isotopic Composition – Atom %			Source
Fuel (as specified)	U-235 – 3.2287	U-238 – 12.9533	Si-28 – 9.9366	Shipping Papers
	Si-29 – 0.5046	Si-30 – 0.3326	Al-27 – 73.0443	
Cladding (wrought 6061 Al Alloy)	Al-27 – 97.8233	Si-28 – 0.6140	Si-29 – 0.0312	Quality Control Report
	Si-30 – 0.0206	Carbon – 1.0536	Fe-54 – 0.0133	
	Fe-56 – 0.2093	Fe-57 – 0.0048	Fe-58 – 0.0006	
	Cr-50 – 0.0049	Cr-52 – 0.0939	Cr-53 – 0.0106	
	Cr-54 – 0.0026	Cu-63 – 0.0811	Cu-65 – 0.0013	
Fuel Element Handle (Cast A356-T6 Al Alloy)	Al-27 – 97.8233	Si-28 – 0.6140	Si-29 – 0.0312	Quality Control Report
	Si-30 – 0.0206	Carbon – 1.0536	Fe-54 – 0.0133	
	Fe-56 – 0.2093	Fe-57 – 0.0048	Fe-58 – 0.0006	
	Cr-50 – 0.0049	Cr-52 – 0.0939	Cr-53 – 0.0106	
	Cr-54 – 0.0026	Cu-63 – 0.0811	Cu-65 – 0.0362	
Grid Plate (1100-Series Al)	Al-27 – 99.9469	Cu-63 – 0.0367	Cu-65 – 0.0164	MatWeb, (1996-2011)
Concrete	H-1 – 16.8018	H-2 – 0.0019	O-16 – 56.2969	MCNP Primer (Brewer, 2009)
	O-17 – 0.0214	Si-28 – 18.7429	Si-29 – 0.9518	
	Si-30 – 0.6274	Al-27 – 2.1343	Na-23 – 2.1365	
	Ca-nat – 1.8596	Fe-54 – 0.0248	Fe-56 – 0.3896	
	Fe-57 – 0.0090	Fe-58 – 0.0012		
Control Rod (Borated Stainless Steel 304)	Fe-54 – 3.6869	Fe-56 – 57.8772	Fe-57 – 1.3366	SS304 from MCNP Primer (Brewer, 2009)
	Fe-58 – 0.1779	Cr-50 – 0.8237	Cr-52 – 15.8843	
	Cr-53 – 1.8011	Cr-54 – 0.4483	Ni-58 – 5.7165	
	Ni-60 – 2.2020	Ni-61 – 0.0957	Ni-62 – 0.3052	
	Ni-64 – 0.0777	Mn-55 – 1.8887	B-10 – 1.5279	
	B-11 – 6.1501			

Table 2.1. Table of Composition of Materials Used in the Model (cont.).

Regulating Rod (Stainless Steel 304)	Fe-54 – 4.0229	Fe-56 – 63.1511	Fe-57 – 1.4584	MCNP Primer (Brewer, 2009)
	Fe58 – 0.1941	Cr-50 – 0.8781	Cr-52 – 16.9327	
	Cr-53 – 1.9200 Ni-60 – 2.3473	Cr-54 – 0.4779 Ni-61 – 0.1020	Ni-58 – 6.0938 Ni-62 – 0.3253	
	Ni-64 – 0.0829	Mn-55 – 2.0133		
Lead	Pb-206 – 24.4422	Pb-207 – 22.4138	Pb-208 – 53.1440	Chart of Nuclides (Lockheed Martin, 2002)
Cadmium	Cd-106 – 1.2500	Cd-108 – 0.8900	Cd-110 – 12.4900	Chart of Nuclides (Lockheed Martin, 2002)
	Cd-111 – 12.8000	Cd-112 – 24.1300	Cd-113 – 12.2200	
	Cd-114 – 28.7300	Cd-116 – 7.4900		
Water	H-1 – 66.6590 O-17 – 0.0127	H-2 – 0.0077	O-16 – 33.3206	Chart of Nuclides (Lockheed Martin, 2002)

The current model incorporates the ENDF/B-VI (.66c) cross section libraries shipped with MCNP version 5 for all isotopes. These libraries were developed by the National Nuclear Data Center at Brookhaven National Laboratory and contain cross sections defined at a temperature of 293.6 K (Los Alamos National Laboratory, 2008).

2.3. MODEL MODIFICATION

The model was originally built in the 101W core configuration. The current core configuration is 120W. This included two major changes. The fuel elements and control rods had been rearranged and the core had been moved slightly further from the thermal column in order to better align it with the beam port. The model was updated by changing the section which places the fuel elements accordingly and changing the transform which aligns the core. Plots of the geometry of the model are shown in Figures 2.1 and 2.2.

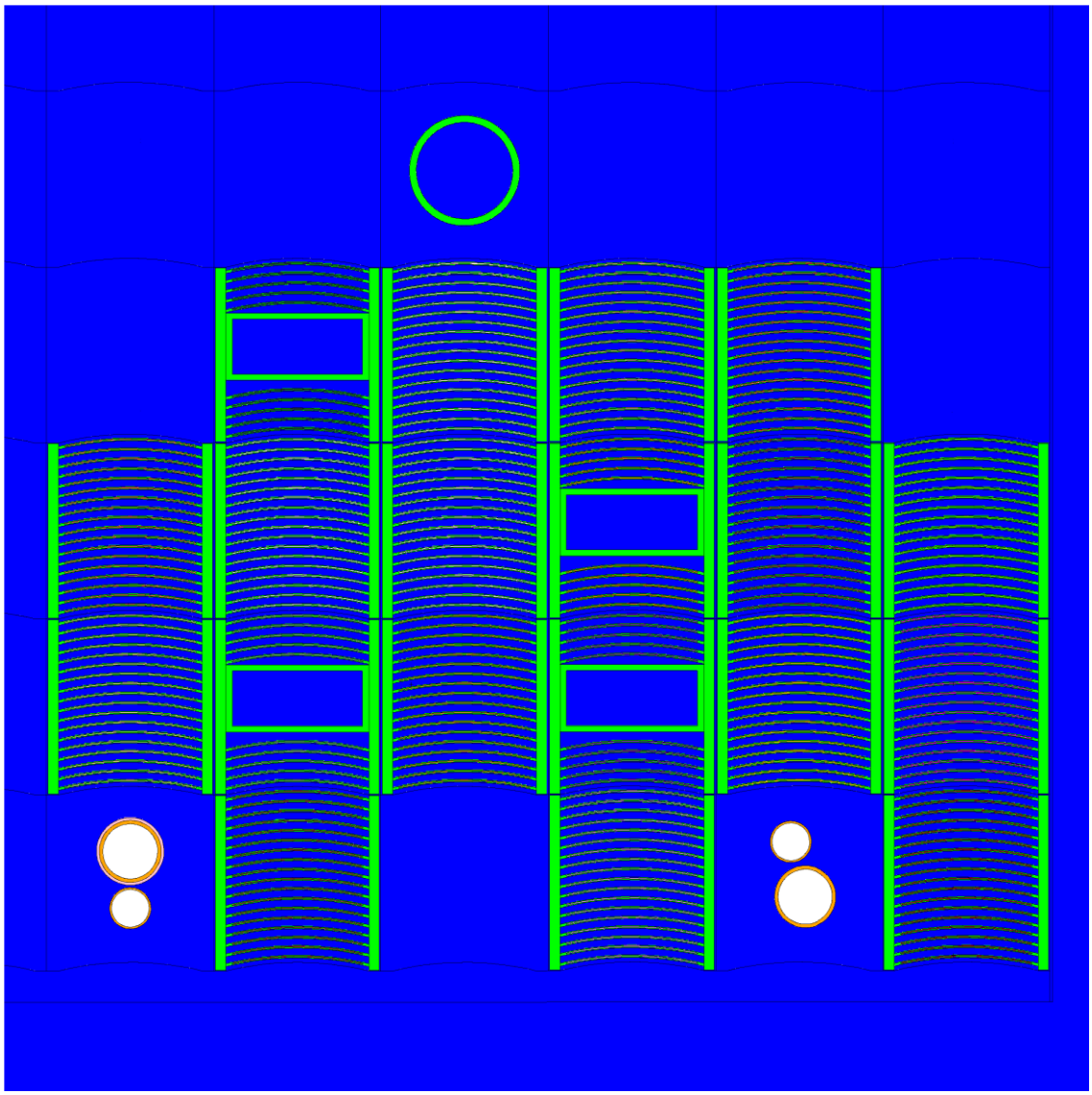

Figure 2.1. xy View of the Model of the Core.

The original model did not include any temperature considerations either. To incorporate this, a temperature definition was added to each cell which contained a material, but not those that were filled by some other cells or universes. Also for any cells that contained water, the density was adjusted to match the density of water at its defined temperature according to a table at engineeringtoolbox.com (Perry & Green, 1997).

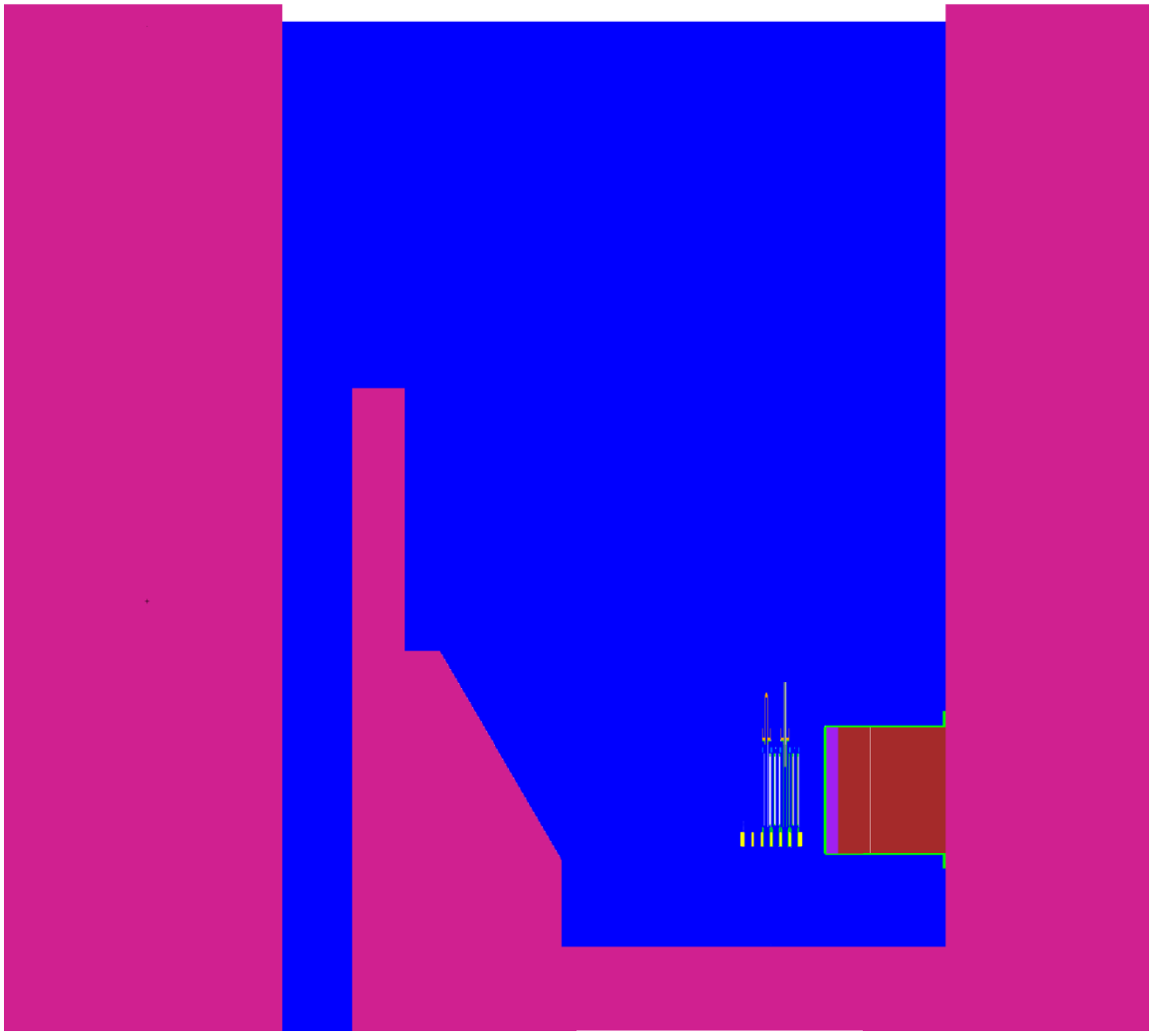

Figure 2.2. yz View of the Model.

As the code was written there was no way to include a temperature difference along the height of the core, so some modifications were made to allow this. The fuel plates and the water between them were divided in half axially, into top and bottom sections. This did not require a restructuring of the code but did require a renumbering to incorporate the additional number of cells.

A copper wire was added to the model in order to measure the flux profile in a similar manner as the experiment performed. This was done by adding a new cell in the base universe and excluding it in the definition of the cell filled by the core. To model the

void coefficient the void tube was added to the model in a similar manner to the fuel elements, so that it could be easily placed around the core. For the approach to criticality simulations the source was added to the source tube universe.

3. SIMULATION

3.1. COMPUTERS USED

In order to run the simulations, a couple different computers were used. For simulations in which only one iteration was needed to collect a set of data, a personal computer running Windows 7 with a dual core processor was used. For simulations needing multiple iterations a computer in the nuclear engineering department running Windows 7 with a hyper-threaded quad core processor was used to allow running of up to 7 simulations simultaneously. In either situation a typical simulation would complete in approximately 8 hours.

3.2. MODERATOR TEMPERATURE COEFFICIENT

In order to model the moderator temperature coefficient of the core, data taken from the NE 308 lab was used. At a given time the control rod positions and temperature at several thermocouples were recorded. The model was adjusted to match the recorded rod heights and temperatures. In any cells containing water the density was adjusted to match its value at that temperature (Perry & Green, 1997). The model was then used to predict the criticality of the system. For one set of data the temperature recorded at the thermocouple above the core was used, and for one set the temperature below the core was used. For these situations the entire model was assumed to be at that temperature. For another set of data the axially divided model was used to allow for a coarse representation of the temperature gradient. For this situation the temperature of the bottom half was set to $T_I + 1/4*(T_O-T_I)$ and the top half was set to $T_I + 3/4*(T_O-T_I)$. Cells located at the top of the core were set to T_O and the rest of the model was set to T_I.

3.3. FLUX PROFILE

In order to compare a measurement of the flux profile in the core to that determined in the model, a copper wire was added to the model. It was placed at the same position in the core as it was placed during the experiment. The wire modeled was 50 in.

long and had a diameter of 0.0225 in., the same as a 14 gauge wire. The material used for this cell was assumed to be pure copper with a ratio of naturally occurring isotopes as given in the chart of nuclides (Lockheed Martin, 2002). A volume flux tally was written for this cell which divided it into 1 in. segments and included a multiplier to give the output as a neutron absorption rate in each segment for a 200 kW core. Three different scenarios were simulated. One in which the model predicted a k_{eff} of 1, one in which the control rods were fully withdrawn, and one in which the core was divided and the same scenario as the first time step in the moderator temperature coefficient experiment was modeled.

3.4. APPROACH TO CRITICALITY

In order to model the approach to criticality experiment the source was added to the model. The dimensions for the source were taken from the documents prepared by the company who produced it. Dimensions for the container were provided, but only amounts of material were provided for the source so it was assumed to be cylindrical, sitting at the bottom of the container. The string holding the source and the ring to which it is attached were omitted and the source was assumed to sit in the middle of the source holder tube. The source was simply added to the source holder element in the model.

In order to simulate the experiment, the control rods were placed in the same position as in the experiment and k_{eff} was calculated. k_{eff} is related to 1/M according to equation 1 (Lamarsh, 2001).

$$\frac{1}{M} = 1 - k_{eff} \tag{1}$$

The critical control rod height was then predicted in the same manner as performed in the experiment. Because the methods for determining k_{eff} in the simulation and the experiment produce drastically different values, only the predictions for the critical control rod height are comparable quantities.

3.5. VOID COEFFICIENT OF REACTIVITY

To simulate the void coefficient of reactivity the void tube was added to the model. The void tube used in the experiment was measured using a tape measure and calipers and those dimensions were used. It was added to the model in the same fashion as a fuel element so as to be easily moved.

The void tube was placed in the same position as in the experiment and the control rods were placed in the same position as when the core was critical. The simulation for the void tube filled with air and the void tube filled with water were both run. For the air filled void tube the air space was taken to be a void as the difference between air and a void is essentially negligible. The k_{eff} of the model was then calculated. Also, the water filled tube with the control rods in the same position as the air filled situation, and the air filled tube with the control rods in the same position as the water filled situation were simulated. This allowed for a direct calculation of the reactivity change due to the void and due to the movement of the control rod.

For the model to accurately predict the void coefficient of reactivity, k_{eff} need not equal 1. The k_{eff} of the water filled and air filled void tube simulations simply need to agree. Also the change in reactivity by changing the tube from water filled to air filled without changing the control rod height should be the same as that calculated in the experiment.

4. EXPERIMENTS

4.1. MODERATOR TEMPERATURE COEFFICIENT

It is difficult to measure the moderator temperature coefficient directly. In order to get some measurement of the effect, the reactor and coolant must be allowed to heat up during the course of operation. In order to perform this experiment, in the morning the pre-startup checklist is performed and the reactor is brought to full power and placed in auto control. This is done in such a manner that the regulating rod is inserted relatively far to allow it to be removed from the core during the course of the experiment. Every 15 minutes during the day, the control rod positions and temperatures of the thermal couples (one placed 5 feet above the core and 2 placed directly below the core) are recorded. Figure 4.1 shows this data. Because the reactivity worth of the control rods is known, a reactivity change due to the heating of the core can be calculated.

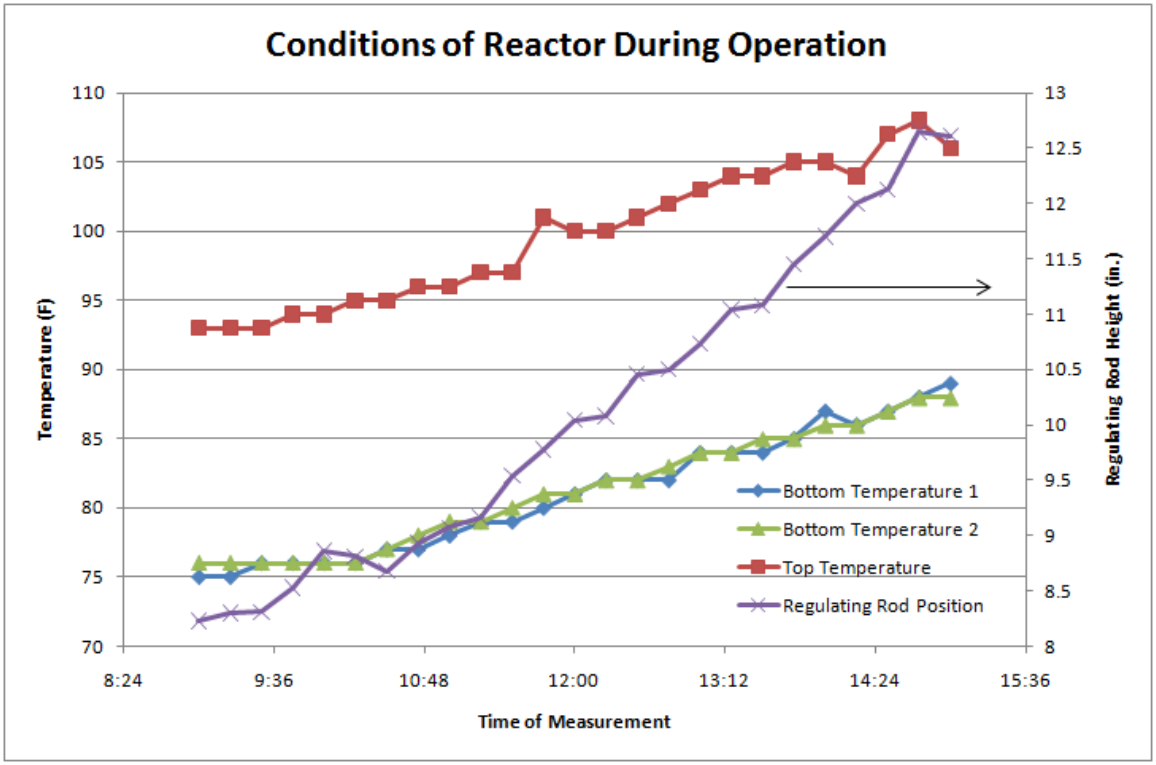

Figure 4.1. Conditions of the Reactor as Recorded During the Moderator Temperature Coefficient Experiment (Shim Rods held at constant height).

4.2. FLUX PROFILE

Because the flux profile of the reactor cannot be measured directly, an experiment was derived to approximate it. A copper wire of known dimensions is placed inside one of the fuel elements and the reactor is brought to 500 W, operated for 10 minutes and then shut down. The wire is removed and allowed to "cool off" such that the shorter lived copper-64 isotope has decayed away. Then the wire is cut into 1 inch long segments and its activity is measured. The activity measured for each segment is divided by its mass, as it is not possible to cut each segment to be identical. It is also then necessary to calculate what the activity of each segment was at the time it was removed from the core, as a significant amount of time passed between the measurement of the first and last segments. Because the activity of each segment is linearly related to the flux in the core, it is assumed that a graph of this data will have the same shape as a graph of the flux profile.

4.3. APPROACH TO CRITICALITY

The goal of this experiment is to predict the height of the control rods when the reactor becomes critical. In order to do this, the pre-startup checklist is performed and the control rods are partially withdrawn. With the neutron source still in place a fission chamber is used to measure the neutron population of the core. The rods are then withdrawn a little more and any transients are allowed to die out. Then another measurement of the neutron population is taken. The k_{eff} of the core can then be predicted based on equations 2 and 3 (Lamarsh, 2001).

$$\frac{1}{M} = \frac{C_0}{C} \tag{2}$$

$$M = \frac{1}{1 - k_{eff}} \tag{3}$$

C_0 is the count rate at the original control rod height and C is the count rate at the current position. A plot of control rod height vs. 1/M is made and a line between the two

points is used to predict the critical control rod height. The predicted critical rod height is the point at which 1/M=0. The control rods are then brought to halfway between the current height and the predicted critical height and the procedure is repeated. A line between the two latest points predicts a new critical rod height and the procedure is repeated until the predictions are within 0.1 in.

4.4. VOID COEFFICIENT OF REACTIVITY

In order to determine the void coefficient of reactivity a series of experiments were performed using the void tube. The void tube is a long, hollow, aluminum cylinder with a removable cap at the top, and a bottom shaped so as to fit into the core grid plate. The tube is filled with water, lowered into a grid space and the reactor is brought to a critical state. The height of the control rods is noted and then the procedure is repeated for several different grid locations. For ease of comparison, the control rods are brought to the same height at each position and the regulating rod is adjusted to make the reactor critical. The experiment is repeated with the void tube filled only with air and the results are compared. Because the reactivity worth of the control rods is known at all positions, the difference in height of the regulating rod needed to make the reactor critical with the void tube filled with air or water directly relates to the reactivity worth of the void.

5. RESULTS

5.1. MODERATOR TEMPERATURE COEFFICIENT

The model was able to predict relatively accurately the effect of the moderator temperature. While the model did not predict the k_{eff} of the core to be 1, it was mostly consistent in its predicted k_{eff} for each method, meaning the effect of raising the regulating rod was offset by changing the temperature in the model. When the high temperature was assumed for the whole core, the over prediction was less than when the lower temperature was assumed. This means that raising the temperature of the model reduces k_{eff}, as it should. The higher temperature model also gave a more consistent prediction than lower temperature model. The lower temperature simulation's fluctuations were still within the noise associated with the type of calculation performed. When the core was divided to simulate a coarse temperature gradient, the model under predicted k_{eff}. Also the model's under prediction was not as consistent. The results for each simulation are shown in Figure 5.1.

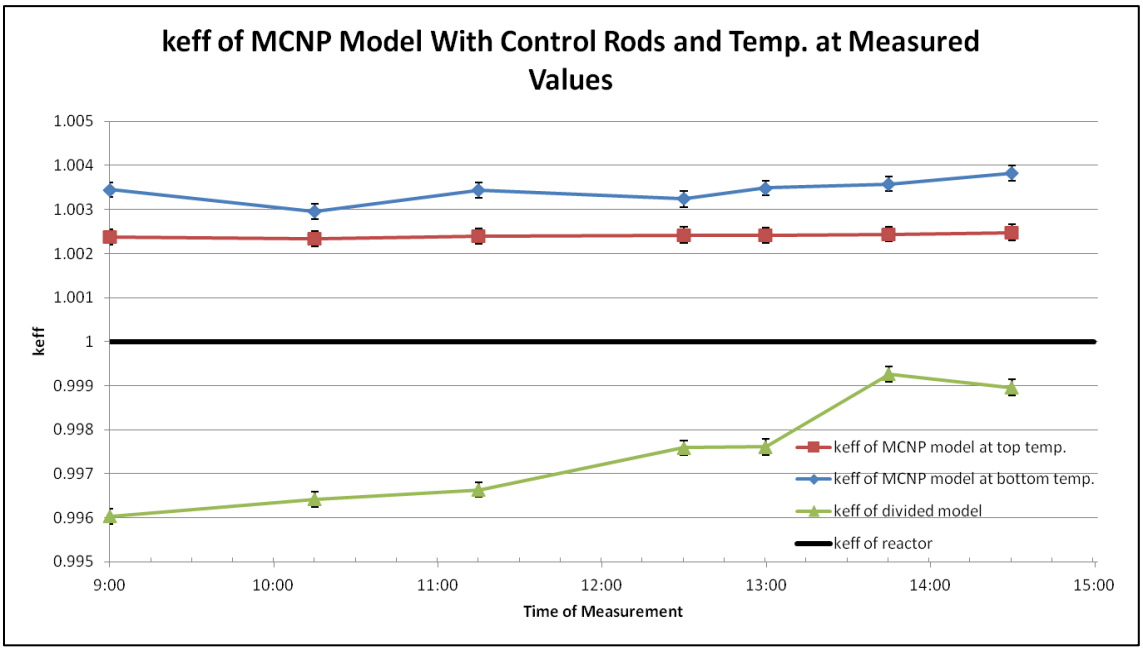

Figure 5.1. Results of Moderator Temperature Coefficient Simulations.

5.2. FLUX PROFILE

In all scenarios modeled, the shape of the neutron flux was similar to the neutron flux measured by experiment. In order to compare the data, each set was normalized to its maximum value. Also, because the exact position of the wire in the experiment was difficult to determine, the data was shifted so that the minimum point before the "wings" matched with the same point as the simulated data. This was assumed to be correct because this phenomenon correlates to the edge of the active core. The flux profiles are graphed in Figures 5.2-5.5.

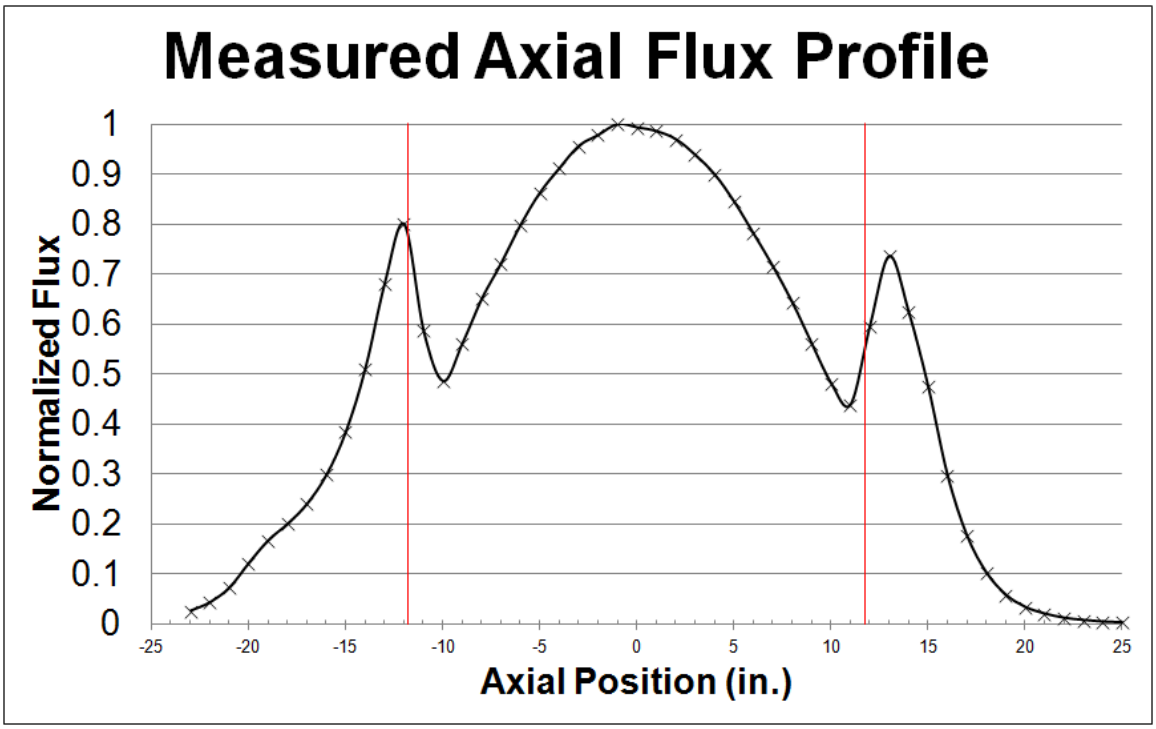

Figure 5.2. Graph of Axial Flux Profile. Positive Position is Up.

The simulated data matches closely to the data from the experiment, most closely is the data set that included the temperature difference along the core. When the control rods are fully withdrawn in the model, the flux profile shifts towards the top, meaning that the control rods are suppressing the flux at the top of the core, as one would expect.

Also, including a temperature difference across the core affects the shape of the flux profile, and including it causes the shape to more closely match the experimental data.

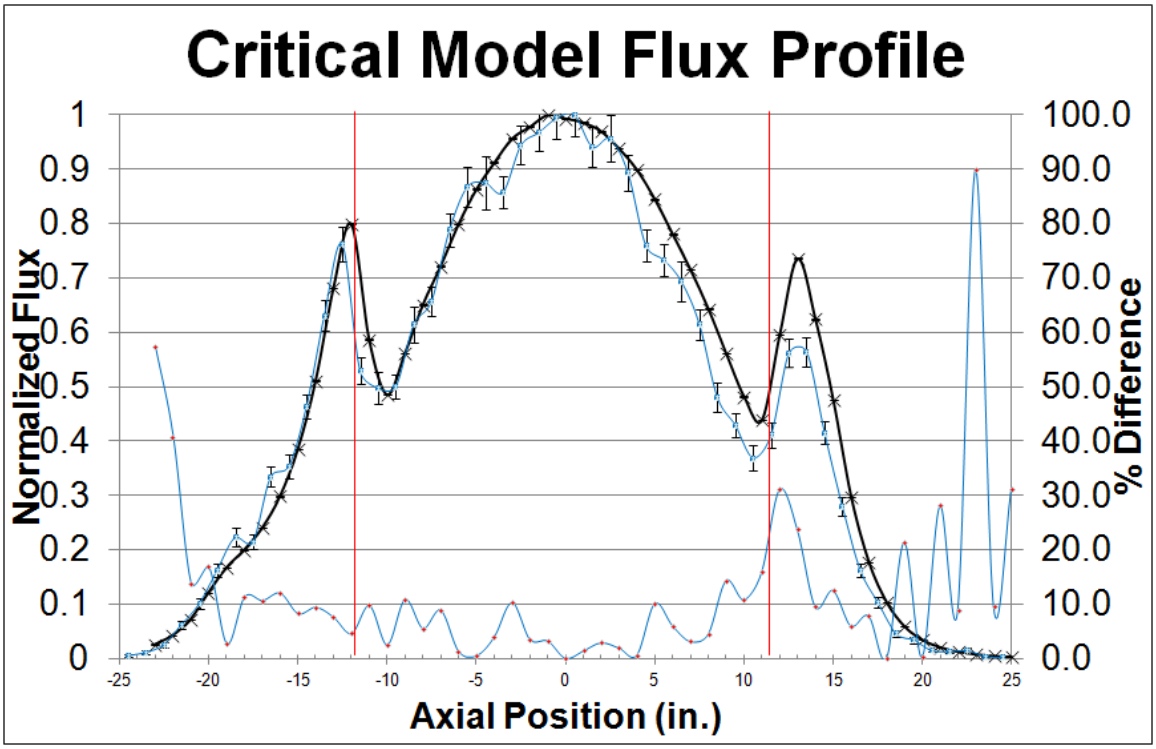

Figure 5.3. Flux Profile Produced by the Critical Model Compared with the Experimental Results.

5.3. APPROACH TO CRITICALITY

The k_{eff} calculated by the model and from the experiment are different. This is due to the fact that in the experiment, 1/M at the first point is equal to 1, i.e. k_{eff} is 0. MCNP calculates a k_{eff} value of 0.96842 for the starting point of 12.5 inch control rod height. The subsequent values are then based on this assumption. This is a consequence of the procedure of the experiment, but does not otherwise affect the calculation of a predicted critical control rod height. The method for predicting critical control rod heights works in both cases and is an accurate and effective tool used historically to safely approach criticality (Stephenson, 1958). The critical control rod height predictions are graphed in Figure 5.6 with respect to the height of the control rods at that step. The critical control

rod height in the model is finally predicted to be 19.3±0.6 in. In the experiment the critical rod height was found to be 20.0 in.

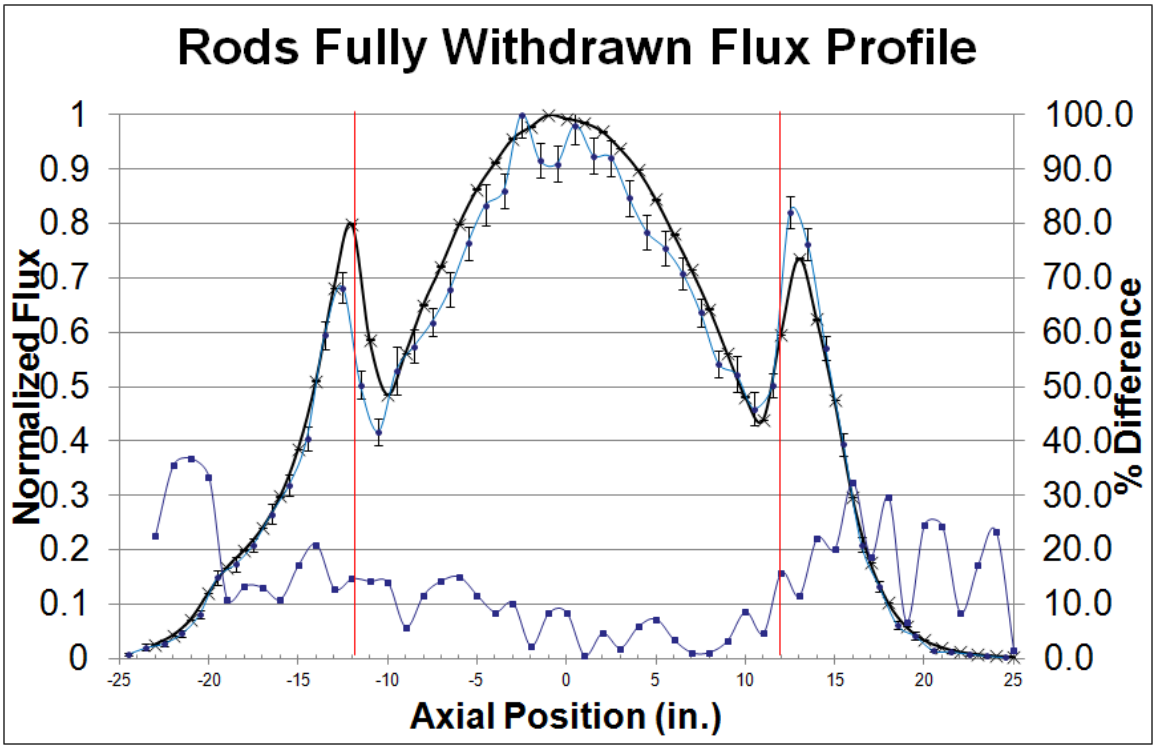

Figure 5.4. Flux Profile Produced by Model with Control Rods Fully Withdrawn Compared with the Experimental Results.

The predicted critical control rod heights from the model and the experiment very nearly match. The slight difference can be attributed to the fact that the model over predicts the criticality of the core slightly, meaning it will predict a lower critical rod height, as seen in the graph.

5.4. VOID COEFFICIENT OF REACTIVITY

The change in reactivity by changing the tube from water-filled to air-filled without changing the control rod heights should be the same as that measured in the experiment, even if k_{eff} is not unity (due to limitations in the model).While the k_{eff}

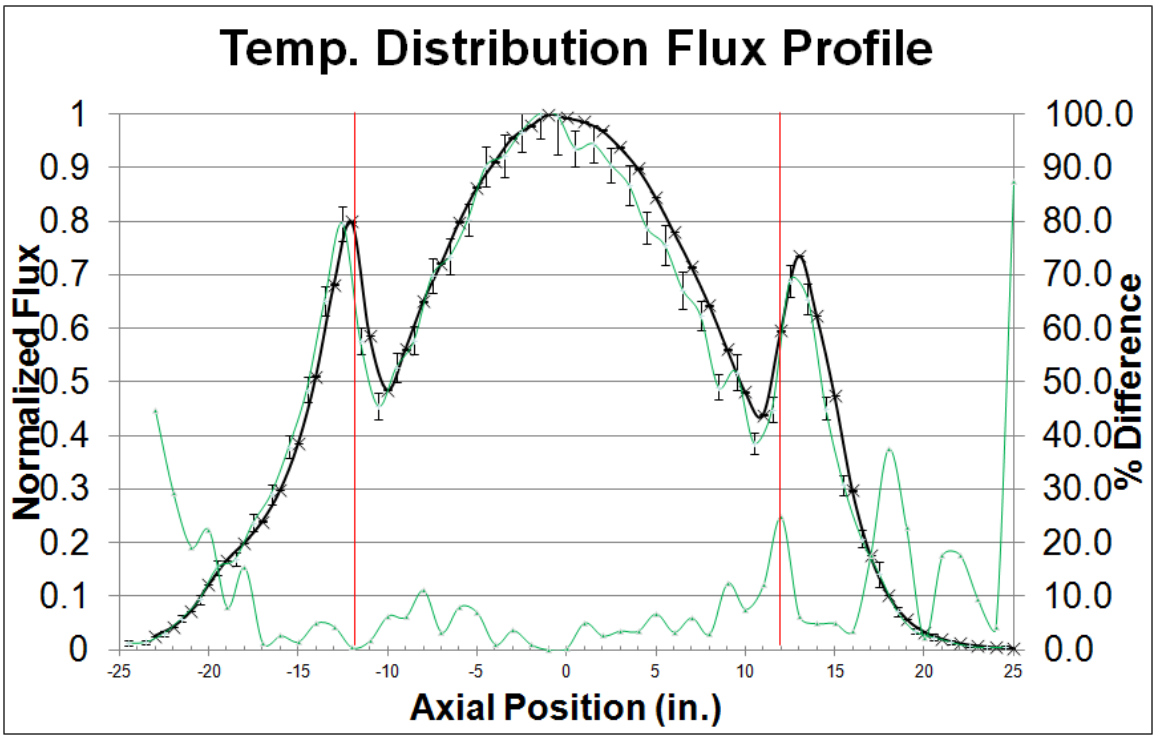

Figure 5.5. Flux Profile Produced by Model with Coarse Temperature Distribution Compared with the Experimental Results.

calculated by MCNP for the air-filled and water-filled void tube cases do not equal one, they do match better than in all cases 0.06%. These values are given in Table 5.1. It is considered that given the current limitations of the model (burnup and temperature effects) the void coefficient of reactivity and its effect on the reactivity of the core is modeled successfully. The k_{eff} calculated from the model is shown in Figure 5.7. Also, the change in reactivity in the model from changing the void tube from water-filled to air-filled without moving the regulating rod matches closely to the value calculated in the experiment, again giving confidence that the void coefficient of reactivity is modeled well. The average value of the void reactivity in the experiment is 0.00142 Δk/k and the average value from the model is 0.00158 Δk/k. Since the volume of the void tube is 1541.22 cm3, the average void coefficient of reactivity of MSTR is 9.24e-7 Δk/k/cm3 in the experiment and 1.02e-6 Δk/k/cm3 in the model. . The values for the reactivity worth of the void are given in Table 5.2. The change in reactivity is also shown in Figure 5.8. We believe that the difference between the simulated and experimental values for each

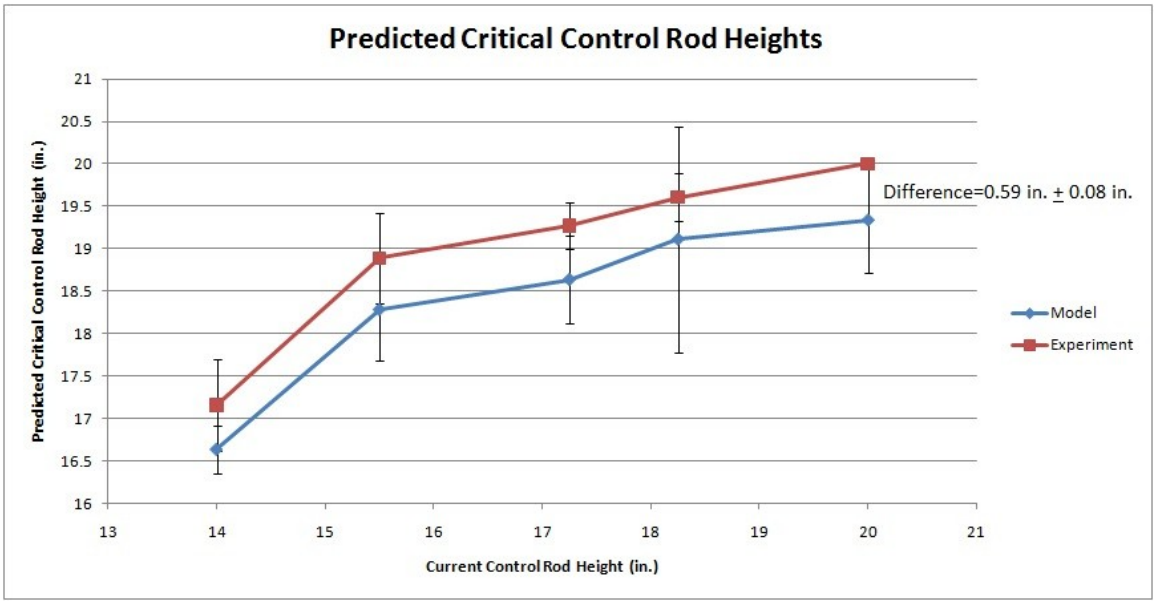

Figure 5.6. Predicted Critical Control Rod Height with Respect to Current Control Rod Height.

Table 5.1. Calculated k_{eff} Values for Modeled Void Tubes.

		Calculated k_{eff}		
Void Tube Position	**Regulating Rod Position (in)**	**Water Filled Void Tube**	**Air Filled Void Tube**	**% Difference**
B7	6.86	1.00132±0.00018		0.020
	16.98		1.00154±0.00018	
B8	6.96	1.00156±0.00018		0.005
	14.03		1.00161±0.00017	
C4	5.98	1.00141±0.00017		0.030
	14.92		1.00167±0.00017	
C9	7.17	1.00185±0.00018		0.060
	18.50		1.00120±0.00017	
D3	6.51	1.00171±0.00017		0.005
	11.67		1.00166±0.00018	

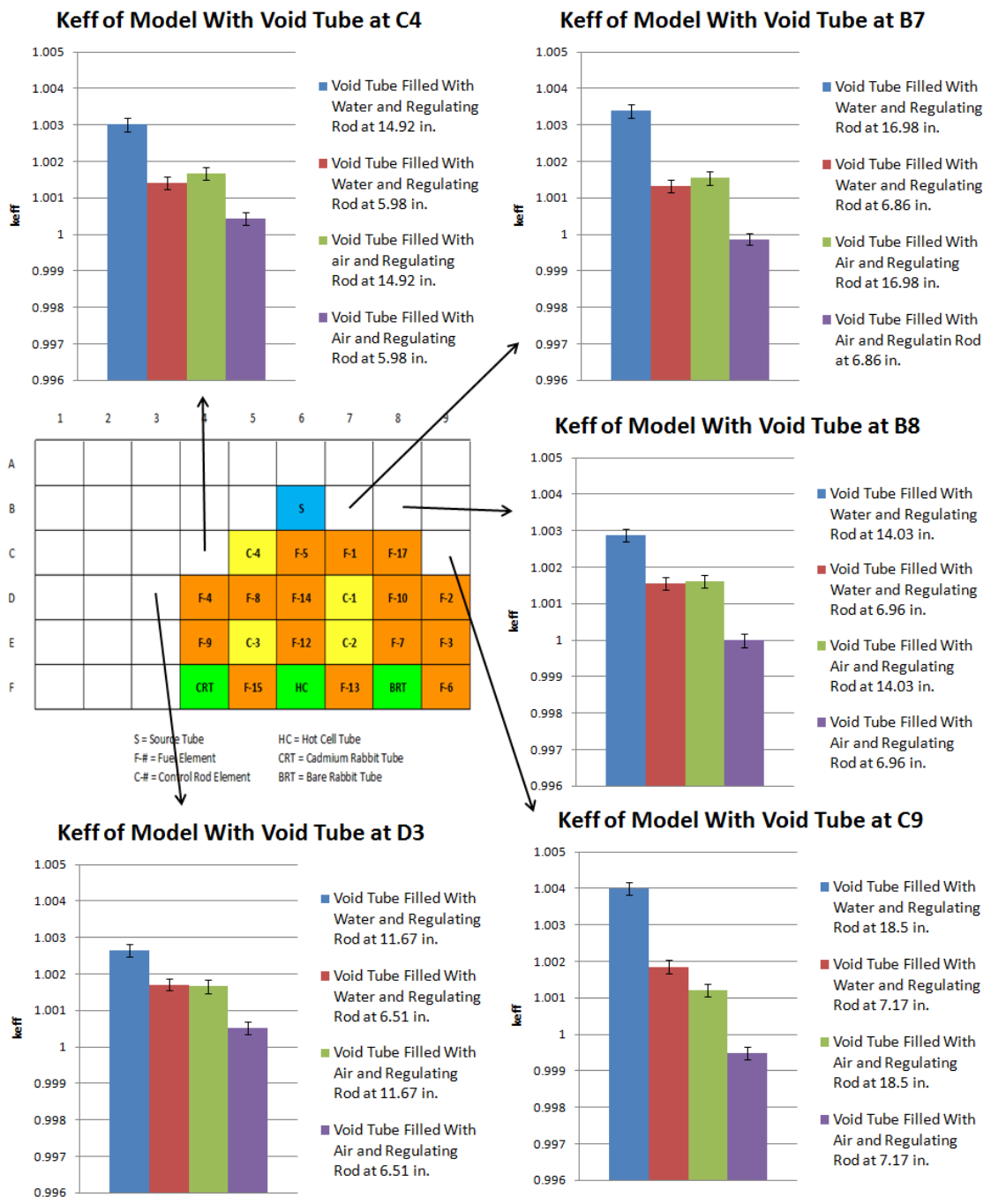

Figure 5.7. k_{eff} Calculated by MCNP with Respect to Void Tube Position; Air-filled and Water-filled Cases with Regulating Rod Positions.

void tube position is due to the way they were determined in the experiment. The differential worth of the regulating rod was determined without the void tube present and

then assumed to have constant values, which is not the case. Unfortunately it is not possible to quantify the effect without recalibrating the regulating rod for each void tube position.

Table 5.2. Reactivity Worth of Void.

		Reactivity of Void (Δk/k)		
Void Tube Position	**Regulating Rod Position (in)**	**Model**	**Experiment**	**% Difference**
B7	6.86	0.00145±0.000248	0.00174	16.7
	16.98	0.00184±0.000255		5.4
B8	6.96	0.00157±0.000255	0.00124	21.0
	14.03	0.00127±0.00024		2.4
C4	5.98	0.00097±0.000240	0.00149	34.9
	14.92	0.00134±0.000248		10.1
C9	7.17	0.00237±0.000255	0.00186	21.5
	18.50	0.00280±0.000248		33.6
D3	6.51	0.00120±0.000240	0.00079	34.2
	11.67	0.00098±0.000255		19.4

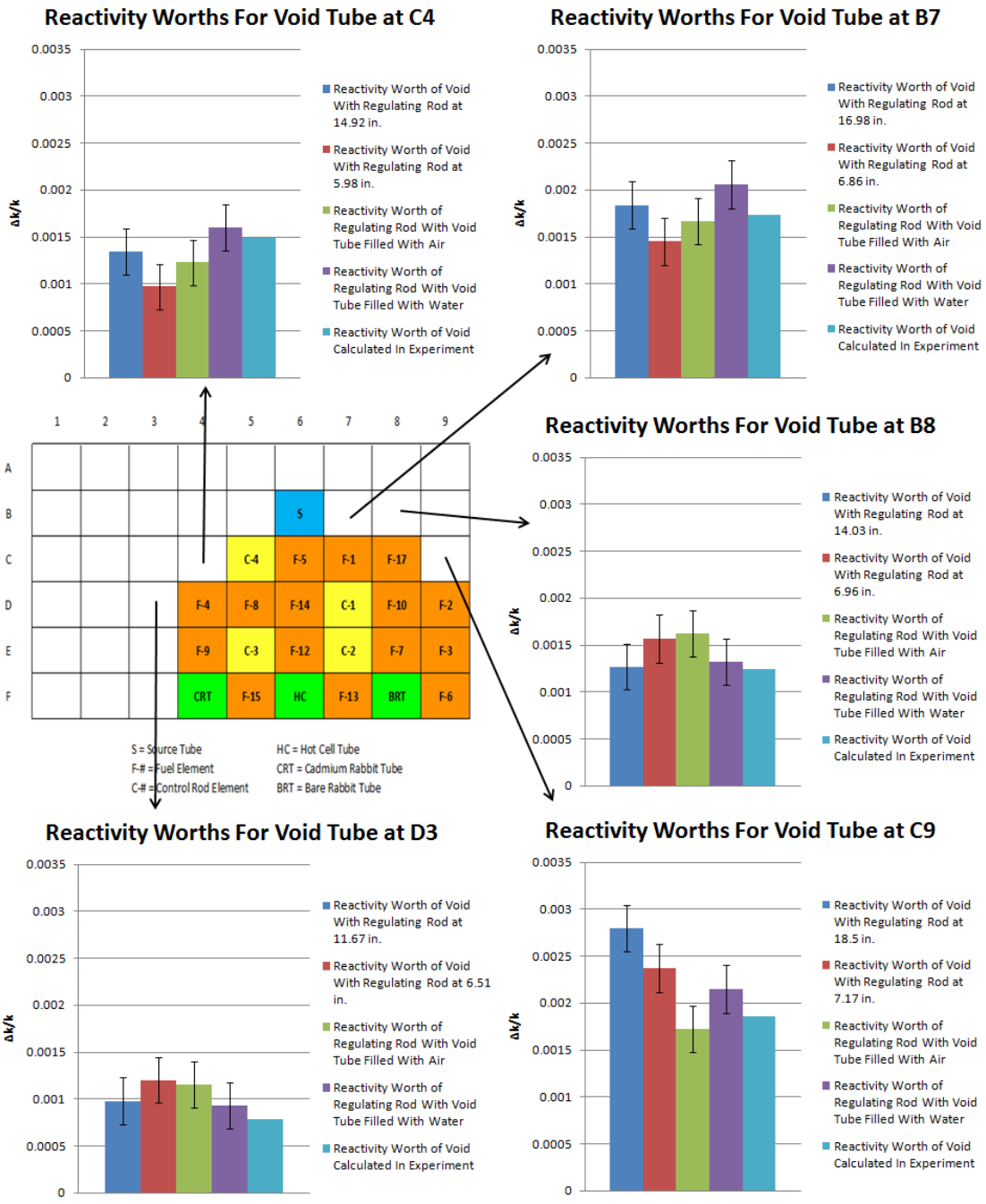

Figure 5.8. Change in Reactivity by Void Tube Position at Various Regulating Rod Positions.

5.5. ERROR ANALYSIS

For the moderator temperature coefficient, the standard deviation of k_{eff} is automatically given by MCNP when k_{eff} is calculated. This was used for the error bars seen on the graph. The core was assumed to have had $k_{eff}=1$ for the duration of the experiment with negligible error, since the reactor was at a stable power.

For the axial flux profile, MCNP automatically calculates the relative error for each tally taken, which is multiplied by the value of the tally to produce the error bars seen on the graph. For the experimental data, the error was calculated using equation 4, where σ_{C_i} is the standard deviation of a particular count and C_i is the value of that count.

$$\sigma_{C_i} = \sqrt{C_i} \tag{4}$$

Then equation 5 gives the standard deviation of counts.

$$\sigma_C{}^2 = \frac{1}{\sum_{i=1}^{n} \frac{1}{\sigma_{C_i}{}^2}} = \frac{1}{\sum_{i=1}^{n} \frac{1}{C_i}} \tag{5}$$

The average background radiation is given by the equation 6, where b_i is one measurement of the background and n is the number of measurements.

$$b = \frac{b_1 + b_2 + \cdots + b_n}{n} \tag{6}$$

Then the standard deviation for the background is given by equation 7.

$$\sigma_b = \sqrt{\frac{b}{n}} \tag{7}$$

The standard deviation for the time of measurement is assumed to be 1 minute and the standard deviation for the measurement of the mass of each segment is assumed to be the accuracy of the scale, which is 0.0005 g. The decay constant for Cu-66, λ, is 0.00091 min^{-1}. The activity of each segment is then given in decays/min./g by equation 8, where C_i is the measured activity of the segment, b is the average background, λ is the decay constant, t is the time after removal from the core that the segment was measured, and m_i is the mass of the segment.

$$A_{0_i} = \frac{(C_i - b)e^{\lambda t}}{m_i} \tag{8}$$

The standard deviation of the activity of each segment is then given by equation 9 (Knoll, 2000).

$$\sigma_{A_{0_i}}{}^2 = \left(\frac{\partial A_{0_i}}{\partial C_i}\right)^2 \sigma_C{}^2 + \left(\frac{\partial A_{0_i}}{\partial b}\right)^2 \sigma_b{}^2 + \left(\frac{\partial A_{0_i}}{\partial t}\right)^2 \sigma_t{}^2 + \left(\frac{\partial A_{0_i}}{\partial m_i}\right)^2 \sigma_m{}^2 \tag{9}$$

Plugging into the formula then gives equation 10.

$$\sigma_{A_{0_i}}{}^2 = \left(\frac{e^{0.00091t}}{m_i}\right)^2 \frac{1}{\sum_{i=1}^{n} \frac{1}{C_i}} + \left(-\frac{e^{0.00091t}}{m_i}\right)^2 \frac{b}{n} + \left(\frac{\lambda(C_i - b)e^{0.00091t}}{m_i}\right)^2 + \left(-\frac{(C_i - b)e^{0.00091t}}{m_i{}^2}\right)^2 \sigma_m{}^2 \tag{10}$$

When calculating the predicted critical control rod height, several measured values had some error involved. For the count rate measured the standard deviation was calculated using equation 11, where n=3, because three measurements were taken.

$$\sigma_{C_i} = \sqrt{\frac{C_{i_{avg}}}{n}} \tag{11}$$

The standard deviation of the control rod height (σ_h) was assumed to be 0.1 in. since that is the accuracy of the control rod height indicator. The formula for predicting the critical control rod height is then given by equation 12, where C_0 is the count rate at 12 in., C_i is the count rate at the current control rod height, C_{i-1} is the count rate at the previous control rod height, h_i is the current control rod height, and h_{i-1} is the previous control rod height.

$$P_{C_i} = \frac{\frac{C_0}{C_{i-1}} - \left(\frac{\frac{C_0}{C_{i-1}} - \frac{C_0}{C_i}}{h_{i-1} - h_i} \right) h_{i-1}}{\frac{\frac{C_0}{C_{i-1}} - \frac{C_0}{C_i}}{h_{i-1} - h_i}} \tag{12}$$

The standard deviation for the predicted critical rod height is then given by equation 13, where the derivatives are given by equations 14-18

$$\sigma_{P_{C_i}}{}^2 = \left(\frac{\partial P_{C_i}}{\partial C_0} \right)^2 \sigma_{C_0}{}^2 + \left(\frac{\partial P_{C_i}}{\partial C_i} \right)^2 \sigma_{C_i}{}^2 + \left(\frac{\partial P_{C_i}}{\partial C_{i-1}} \right)^2 \sigma_{C_{i-1}}{}^2 + \left(\frac{\partial P_{C_i}}{\partial h_i} \right)^2 \sigma_{h_i}{}^2 + \left(\frac{\partial P_{C_i}}{\partial h_{i-1}} \right)^2 \sigma_{h_{i-1}}{}^2 \tag{13}$$

$$\frac{\partial P_{C_i}}{\partial C_0} = 0 \tag{14}$$

$$\frac{\partial P_{C_i}}{\partial C_i} = \frac{C_{i-1}(h_i - h_{i-1})}{(C_{i-1} - C_i)^2} \tag{15}$$

$$\frac{\partial P_{C_i}}{\partial C_{i-1}} = \frac{C_i\left(h_{i-1} - h_i\right)}{\left(C_{i-1} - C_i\right)^2} \tag{16}$$

$$\frac{\partial P_{C_i}}{\partial h_i} = \frac{C_i}{C_{i-1} - C_i} \tag{17}$$

$$\frac{\partial P_{C_i}}{\partial h_{i-1}} = -\frac{C_{i-1}}{C_{i-1} - C_i} \tag{18}$$

The equation for predicting the critical control rod height for the model is given by equation 19, where k_{eff_i} is the multiplication factor at the current control rod height and $k_{eff_{i-1}}$ is the multiplication factor at the previous control rod height.

$$P_{C_i} = \frac{\left(1 - k_{eff_{i-1}}\right) - \left(\frac{\left(1 - k_{eff_{i-1}}\right) - \left(1 - k_{eff_i}\right)}{h_{i-1} - h_i}\right) h_{i-1}}{\frac{\left(1 - k_{eff_{i-1}}\right) - \left(1 - k_{eff_i}\right)}{h_{i-1} - h_i}} \tag{19}$$

The control rod height is precisely defined in the model so σ_h for the model is 0. This gives equation 20 for the standard deviation of predicted control rod height for the model, where the derivatives are given by equations 21 and 22.

$$\sigma_{P_{C_i}}{}^2 = \left(\frac{\partial P_{C_i}}{\partial k_{eff_i}}\right)^2 \sigma_{k_{eff\,i}}{}^2 + \left(\frac{\partial P_{C_i}}{\partial k_{eff_{i-1}}}\right)^2 \sigma_{k_{eff\,i-1}}{}^2 \tag{20}$$

$$\frac{\partial P_{C_i}}{\partial k_{eff_i}} = \frac{\left(k_{eff_{i-1}} - 1\right)\left(h_{i-1} - h_i\right)}{\left(k_{eff_{i-1}} - k_{eff_i}\right)^2} \tag{21}$$

$$\frac{\partial P_{C_i}}{\partial k_{eff_{i-1}}} = -\frac{\left(k_{eff_i} - 1\right)\left(h_{i-1} - h_i\right)}{\left(k_{eff_{i-1}} - k_{eff_i}\right)^2} \tag{22}$$

For modeling the void coefficient of reactivity, the change in reactivity was simply calculated using equation 23, where k_1 and k_2 are the multiplication factors calculated by MCNP for different situations.

$$\Delta k = k_1 - k_2 \tag{23}$$

The equation for the standard deviation is then given by equation 24.

$$\sigma_{\Delta k} = \sqrt{\sigma_{k_1}{}^2 + \sigma_{k_2}{}^2} \tag{24}$$

For the void coefficient experiment, an analysis of the error involved was not possible due to the multiple unknown factors involved in its calculation. The values used for the worth of the regulating rod at various heights were interpolated from a nonlinear table of values with unknown errors. It is believed that the error for the calculation of the reactivity change due to the void would be significant, but due to the inability to calculate it, it was not included.

6. CONLUSIONS

6.1. DISCREPANCIES BETWEEN SIMULATION AND EXPERIMENT

The majority of the discrepancies between the experimental and simulated data can be attributed to the fact that the model uses fresh fuel, and thus over-predicts k_{eff} for nearly all of the simulations. The slight difference of the axial profile is attributed to the effect of the control rods being at slightly different heights and the temperature profile of the core not being modeled except in the one case, which caused it to match much more closely.

6.2. POSSIBLE SOURCES OF ERROR

The over prediction of k_{eff} by the model when simulating the moderator temperature coefficient is likely the result of using fresh fuel composition. The under prediction when a temperature gradient was simulated could be the result of multiple different assumptions. First, the temperature gradient is simulated using only two sections along the length of the core. Also it was assumed that the temperatures measured by the thermocouples were the temperatures directly at the top and bottom of the core, which is likely not the case, because the thermocouples are not directly next to the core, especially not the one above the core. A linear temperature gradient was assumed, which is also not necessarily the case. Finally, the fuel and cladding were assumed to be at the same temperature as the water between them, which will not be the case.

There is little discrepancy between the flux profile measured experimentally and that determined by the simulation. However, it can be seen that both the control rods and the temperature gradient do have some effect on the shape of the flux profile, and that in order to best predict it both should be taken into account.

The k_{eff} calculated using MCNP and that calculated from the experiment in the approach to criticality experiment are dramatically different. This is due to the fact that in the experiment, 1/M at the first point is taken to be equal to 1, i.e. k_{eff} is assumed to be 1. In the experiment the core is assumed to have a 1/M value of 1 with the control rods at 12.5 in., corresponding to a value for k_{eff} of 0, whereas MCNP calculates a k_{eff} value of

0.96842. The subsequent values are then based on this assumption. The experiment and the model do however predict very similar critical rod heights. The difference in their predicted critical control rod heights can be attributed to the fact that the model over predicts k_{eff} when a critical configuration is used, meaning that it should predict a critical control rod height slightly lower than found by the experiment.

For the void coefficient of reactivity there is some discrepancy at position C9, but it is believed that this is due to the attempt to compensate for the change in reactivity in a different part of the core. Also, in the experiment, the effect of the void on the worth of the control rod was not taken into account when calculating the reactivity effect of the void.

7. FUTURE WORK

7.1. UPDATE FUEL COMPOSITION

The fuel composition of the model is currently taken as fresh fuel. The current fuel is nearing 20 years of operation and thus has been depleted of U-235 and now includes some fission products. It has been seen that this causes some significant discrepancy between experimental and simulated results. In the interest of using as accurate a model as possible, the composition of the fuel and possibly some of the other materials in the core should be updated to match as near as possible the current composition of the core.

7.2. PERFORM HEAT TRANSFER AND FLUID FLOW ANALYSIS

The simulations performed thus far have assumed the fuel to be the same temperature as the coolant. This is most certainly not the case in an operating reactor. Also the temperatures used were measured some distance from the core and thus may not accurately represent the actual temperatures within the core. A fluid flow and heat transfer analysis of the core should be performed to accurately predict the temperature of the fuel, cladding, and water between the plates so that this can be incorporated into the model.

7.3. MODEL DESIRED UPGRADES

Once the model has been updated to better reflect the actual conditions within the core, it should be used in conjunction with a heat transfer and fluid flow analysis to predict the effects of increasing the power and installing a secondary cooling system. Once all of the analysis has been completed, a compelling case will have been made for the NRC to allow these upgrades.

BIBLIOGRAPHY

Bonzer, B. (2011, March). Reactor Director. (B. Richardson, Interviewer)

Brewer, R. (2009). *Criticality Calculations with MCNP5: A Primer.*

Grant, E. J., Mueller, G. E., Castano, C. H., Kumar, A. S., & Usman, S. (2010). *Internet Accessible Hot Cell with Gamma Spectroscopy at the Missouri S&T Nuclear Reactor.* American Nuclear Society Transactions.

Knoll, G. F. (2000). *Radiation Detection and Measurement.* John Wiley & Sons, Inc.

Lamarsh, J. R. (2001). *Introduction to Nuclear Engineering.* Prentice Hall.

Lockheed Martin. (2002). *Nuclides and Isotopes.* Lockheed Martin Distribution Services.

Los Alamos National Laboratory. (2008). *MCNP — A General Monte Carlo N-Particle Transport Code, Version 5.*

MatWeb. (1996-2011). *MatWeb*. Retrieved 2011, from MatWeb.

Missouri S&T Nuclear Reactor. (2008). Retrieved 2011, from Missouri University of Science and Technology: http://nuclear.mst.edu/research/reactor.html

Perry, R. H., & Green, D. W. (1997). *Perry's Chemical Engineers' Handbook.* McGraw-Hill Professional.

(1988). *Safety Analysis Report For The University of Missouri-Rolla Reactor.*

Stephenson, R. (1958). *Introduction to Nuclear Engineering.* McGraw-Hill Book Company.

VITA

Bradley Paul Richardson was born to parents Robert and Lisa Richardson. He attended Fleetridge Elementary in Raytown, MO before moving to Richmond, MO in 1996. In 2001 he earned his Eagle Scout Award, and in 2005 graduated from Richmond High School. That fall he began school at the University of Missouri-Rolla, and joined Sigma Pi Fraternity.

In May, 2009, Brad graduated with a Bachelor of Science in Nuclear Engineering from what is now Missouri University of Science and Technology. He then enrolled in Graduate School at Missouri S&T and was awarded the Chancellor's Fellowship. He will have completed his Masters in Nuclear Engineering in December, 2012.

Brad is currently employed at Transware Enterprises as a level 1 Nuclear Engineer. Transware is a consulting firm which provides best estimate fluence calculations to operating power plants as well as fuel selection packages for dry cask storage.